Surface Chirality

DOI: 10.1002/ange.200501655

Enantiospecific Chemisorption of Small Molecules on Intrinsically Chiral Cu Surfaces**

*Bhawna Bhatia and David S. Sholl**

Solid surfaces that define chiral interfaces are of great interest for potential applications in chiral processing.[1–4] The observation that highly stepped metal surfaces are intrinsically chiral has created interest in the use of these surfaces for enantiospecific separations and catalysis.[5–9] An enantiospecific separation based on the reversible adsorption of molecules on a chiral Cu surface has recently been demonstrated.[10] Chemisorption of enantiopure amino acids on low-index Cu surfaces has been shown to lead to the spontaneous formation of homochiral surface facets.[11] A number of common mineral surfaces are also intrinsically chiral.[12] Enantiospecific adsorption on chiral surfaces is controlled by the preferred locations and orientations of adsorbed molecules, but assessment of these properties experimentally is extremely challenging. Below, we present predictions of the preferred binding configurations of two small species on a chiral Cu surface, Cu(874), made by using density functional theory (DFT) calculations.

Previous theoretical studies of molecular adsorption on chiral metal surfaces have focused on physisorbed molecules, which can be described using empirical potentials.[6,8,9,13] DFT has been used to study the chemisorption of $HSCH_2CHNH_2CH_2P(CH_3)_2$ on a chiral Au surface,[14] thus predicting a binding-energy difference between the two molecular enantiomers of 0.09 eV. Unfortunately, neither this molecule nor the Au surface used in these calculations have been characterized experimentally. Herein, we consider a chiral Cu surface of the type that has been used in a number of experiments[15–18] and examine two molecular adsorbates, one of which, propylene oxide, has been used in several experimental studies of surface chirality.[1,16,19] We recently used DFT methods very similar to those used below to determine the structure of chiral adlayers of amino acids on low-index Cu surfaces and found very good agreement between the calculated structures and those observed experimentally.[20,21]

Our calculations examined the adsorption of the amino-(fluoro)methoxy (FAM) species and propylene oxide on a Cu(874) surface. A schematic view of these moieties as they bind on Cu surfaces is shown in Figure 1. Cu(874) is intrinsically chiral because of the kinked steps that separate its (111)-oriented terraces (Figure 2).[5–9] Using the standard notation for defining the chirality of these surfaces,[5–9] the surface shown in Figure 2 and used in our calculations is denoted Cu(874)^S. Real chiral Cu surfaces exhibit a distribution of step and kink lengths because of the thermal motion of step-edge atoms.[22,23] Detailed models of these step distributions suggest that the structures that define Cu(874) are representative of a large number of surface orientations with (111)-oriented terraces.[13,24] Cu(643), which has been used in most experiments of intrinsically chiral metal surfaces, also has (111)-oriented terraces.[10] The unit cell of Cu(874) is somewhat larger than Cu(643), thus making it more suitable for calculations in which the effect of adsorbate–adsorbate interactions is minimal.

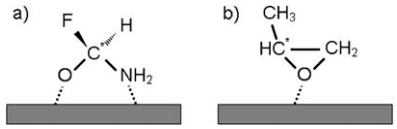

Figure 1. Schematic representations of a) FAM and b) PO binding on a metal surface. In each species, the chiral center is denoted by an asterisk and bonds with the surface are shown with dashed lines.

A challenging aspect of examining molecular adsorption on stepped metal surfaces computationally is that large numbers of adsorption configurations must be examined.[14,18] This task can be simplified if some information is available on

[*] B. Bhatia, Prof. D. S. Sholl
Department of Chemical Engineering
Carnegie Mellon University
Pittsburgh, PA 15213 (USA)
Fax: (+1) 412-268-7319
E-mail: sholl@andrew.cmu.edu

[**] Financial support from the National Science Foundation (CTS-0216170), the US Department of Energy (DE-FG02-03ER15473), and the Alfred P. Sloan Foundation (DSS) is gratefully acknowledged.

Supporting information for this article is available on the WWW under http://www.angewandte.org or from the author.

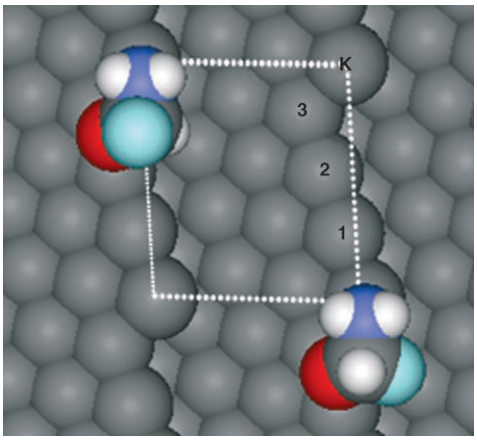

Figure 2. The most favorable binding geometries of *R*-FAM (top left) and *S*-FAM (bottom right) on Cu(874)^S as computed by using DFT. Dashed lines indicate a single surface unit cell. The surface-kink atom (K) and step-edge atoms (1–3) are labeled.

the types of binding sites preferred by the moieties of interest. We first examined the adsorption of methoxy (OCH_3), chlorofluoromethoxy (OCHClF), methylamine (H_3CNH_2), and chlorofluoromethylamine ($HClFCNH_2$) species on Cu(111) (see the Supporting Information). We previously used DFT to examine the adsorption of fluoroethoxy species on Cu(111) and found excellent agreement between the calculated and experimental adsorption geometries and energies.[25] Both methoxy (amine) species were found to favor threefold fcc (top) sites, with each forming a single bond with the surface. We then examined the adsorption of chlorofluoromethoxy and chlorofluoromethylamine species on Cu(874) for multiple positions of these species near the step edge; both favor adsorption on the upper edge of the surface step. Binding energies on the stepped surface were 0.33–0.40 eV more stable than on Cu(111). Based on this observation, we only consider configurations with molecules bound to step edges in the calculations described below. The difference between the binding energy of terrace and step sites is larger for the amine than the methoxy species. The preferred binding site for the amine is on top of the kink atom shown in Figure 2.

Based on our preliminary calculations, we investigated the adsorption of *R*- and *S*-FAM on Cu(874)^S in detail. For *S*-FAM, we considered configurations with the amino group on top of atoms K, 1, 2, and 3 in Figure 2. For each configuration, six distinct rotations of the N–O direction about the surface normal were considered. For each of these configurations, two distinct orientations that differ in the angle formed by C–H and C–F with respect to the surface normal were examined. This procedure yields 48 distinct configurations for *S*-FAM/Cu(874)^S. An equivalent set of 48 configurations for *R*-FAM was also examined. From these 96 configurations, we excluded 64 states in which the O atom was located in what could be considered a pure terrace site. The remaining 32 states were geometrically optimized by using $3\times3\times1$ *k* points. The 21 states with the most favored energies from these calculations were further optimized with $7\times7\times1$ *k* points and dipole corrections.

Two views of the most favored adsorption configurations for *S*- and *R*-FAM on Cu(874)^S are shown in Figures 2 and 3. There is a significant energy difference between the two

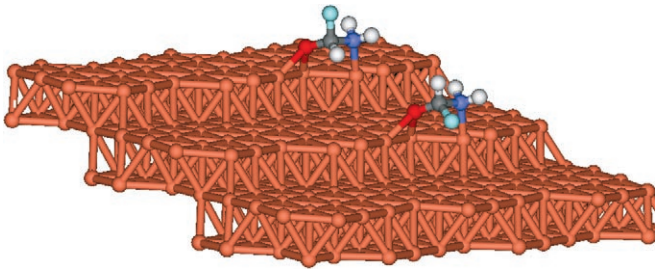

Figure 3. Side view of *R*- (left) and *S*-FAM (right) on Cu(874)^S.

enantiomers, as the *R*-FAM binding to the surface is 0.13 eV stronger than the *S*-FAM binding. This difference is the largest enantiospecific adsorption-energy difference that has been predicted or observed to date for molecular adsorption on a chiral metal surface. The origin of this enantiospecific binding can be understood as follows: Both enantiomers bind to the same surface atoms (see Figure 3). These bonds, as characterized by the Cu–O and Cu–N distances (see the Supporting Information), are essentially the same for the two adsorbed enantiomers. These surface bonds constrain the C–F bond to point towards (away from) the surface for *S*-FAM (*R*-FAM) and vice versa for the C–H bond. The energy difference between the adsorbed enantiomers arises from the different local environments of the F atom; the more stable *R* enantiomer has the F atom far from the surface. The energetic preference for F atoms to not lie close to a Cu surface has been observed before with DFT calculations and experiments for 2-fluoroethoxy/Cu(111).[25] Interactions between the F atom and step edge in *S*-FAM induce slight distortions in the molecule; the O-C-F bond angle is 114° for adsorbed *S*-FAM but 109° for *R*-FAM.

Many local minima exist for *R*- and *S*-FAM on Cu(874)^S. For *R*-FAM, the next four most favorable states had energies of 0.12, 0.18, 0.20, and 0.22 eV relative to the most stable state. For *S*-FAM, the next four locally stable states had energies of 0.16, 0.19, 0.21, and 0.23 eV relative to the favored configuration of *R*-FAM. The distribution of energy minima accessible to each adsorbed enantiomer is shown in Figure 4.

The species treated above exhibits strongly enantiospecific binding on Cu(874)^S but suffers from the serious drawback that it is not readily available for experiments. To address this point, we performed similar calculations for propylene oxide (PO) on Cu(874)^S. PO has previously been used experimentally as a probe for enantiospecific binding on both intrinsically chiral metal surfaces[16] and chirally templated surfaces.[1,19] We first examined the adsorption of PO on Cu(111) and found that the molecule favors a configuration in which the terminal methyl group is oriented away from the surface. Test calculations with PO on Cu(874)^S showed that PO binds much more strongly to step-edge sites than to terrace sites, so only adsorption configurations with the molecule above the step edge were considered

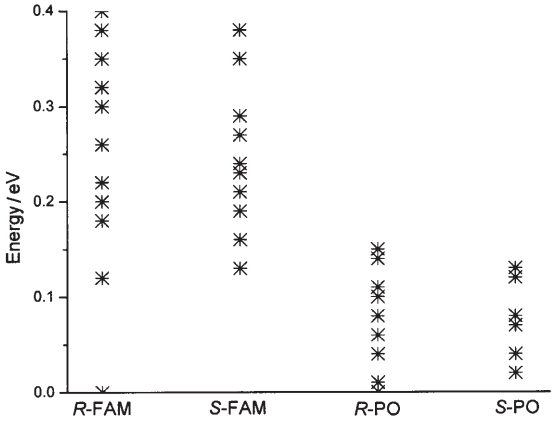

Figure 4. Energies of the distinct local minima observed for FAM and PO adsorbed on Cu(874)^S measured relative to the energy of the most favorably bound configuration of either enantiomer of the species of interest. These results are from calculations using $3\times3\times1$ *k* points. Calculations using $7\times7\times1$ *k* points were performed for 21 states of FAM and 15 states of PO; the figure does not change appreciably if these energies are plotted.

further. A set of configurations sampling the placement and orientation of *S*- and *R*-PO were examined by using methods analogous to our calculations for FAM. In all, 23 configurations were examined. The most stable orientations for each enantiomer on the surface are shown in Figures 5 and 6. Both

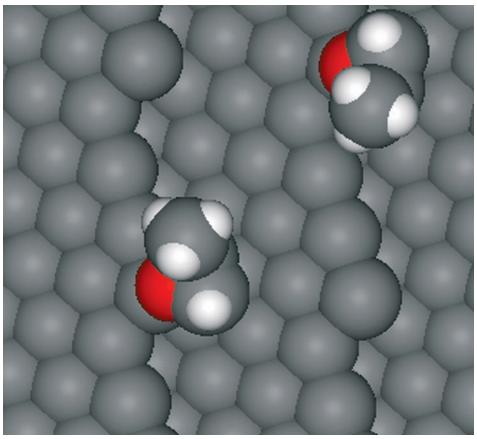

Figure 5. The most favorable binding geometries of *R*- (bottom left) and *S*-PO (top right) on Cu(874)^S, as computed by using DFT.

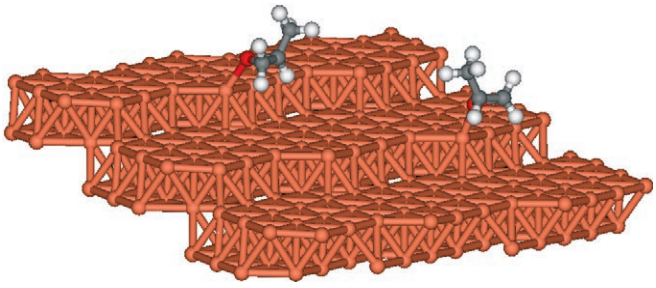

Figure 6. Side view of *R*- (left) and *S*-PO (right) on Cu(874)^S.

enantiomers favor geometries with the O atom above the surface-kink atom and the terminal methyl group oriented away from the surface. The calculated energy difference between the two adsorbed enantiomers is much smaller than the energy difference for FAM; for PO, the energy difference is 0.02 eV with the *R* enantiomer being favored. Energy differences of this magnitude lie close to the limit of those that can be reliably distinguished with DFT, but the distinct orientations of the adsorbed molecules in Figure 5 and the other less favored adsorption configurations described below make it clear that the adsorption of PO on Cu(874)^S is enantiospecific. The energy differences between adsorbed enantiomers of PO are considerably smaller than those described above for FAM. This difference can be understood by noting that the enantiomers differ by which atom, F or H, interacts with the step edge for FAM in its favored configurations. For PO, the same atoms, both H, interact with the step edge for both adsorbed enantiomers, which strongly limits the size of the energy difference between the adsorbed enantiomers.

Similar to FAM, multiple local minima exist for PO on Cu(874)^S, as shown in Figure 4. Because of the relatively small energy differences between these minima, a distribution of states would be observed in any experiment that probes these species. This observation is consistent with the experimental observation that thermal desorption spectra from the most strongly bound surface states of *R*- and *S*-PO on Cu(643) yield broad features that cannot be readily analyzed in terms of adsorption enantiospecificity.[16] Desorption from other surface sites associated with higher surface coverages of PO has been seen experimentally to be enantiospecific.[16] We have not attempted to characterize these states computationally, as it would require the examination of large numbers of coadsorption configurations.

Our DFT calculations have provided two examples of the enantiospecific adsorption of small molecules on a chiral Cu surface, Cu(874)^S. Calculations of this type will be a great assistance to complement experimental studies of molecular adsorption on chiral surfaces.[10–12] By examining the adsorption of a variety of functional groups on stepped metal surfaces, DFT calculations can be used to understand what aspects of molecular architecture can lead to highly enantiospecific interactions with chiral metal surfaces. Similarly, performing analogous calculations on a range of chiral surfaces will provide insight into the role of surface structure on enantiospecific adsorption.[10]

Experimental Section

Our plane-wave DFT calculations were performed with the Vienna ab initio Simulation Package with the ultrasoft pseudopotentials available in this package.[26,27] The results reported above used the generalized gradient approximation (GGA) with the PW91 functional. A small number of configurations were also examined with the rPBE functional within the PAW formalism. The energy differences between configurations with the rPBE-PAW calculations were found to coincide with those of the GGA-PW91 calculations. All GGA calculations used a plane-wave expansion with a cutoff of 425 eV and Fermi-level smearing with a width of 0.2 eV. Geometries were relaxed until the forces on all unconstrained atoms were less than 0.03 eV Å^{-1}.

Final results were computed using a $7 \times 7 \times 1$ *k*-point mesh and dipole corrections. Prior to these calculations, the most favorable configurations were determined using $3 \times 3 \times 1$ *k* points as described above.

In our calculations, the DFT-optimized lattice parameter for Cu was used to define the periodicity of the material in the plane of the surface. The computational supercell contained a single surface unit cell of $Cu(874)^S$ with a vacuum spacing greater than 10 Å in the direction of the surface normal. The surface unit cell is shown in Figure 2. This computational supercell contains 32 metal atoms. Our calculations were performed using slabs equivalent in thickness to three (111)-oriented layers. Molecules were adsorbed on only one side of the slab, and all degrees of freedom of all the metal atoms and the molecule were allowed to relax in all energy minimization calculations. A limited number of calculations, in which all the metal atoms were constrained in their bulk positions, indicated that surface relaxation is not a dominant effect in the relative adsorption energies of the most stable molecular configurations we examined.

Received: May 13, 2005
Revised: July 28, 2005

Keywords: chemisorption · density functional calculations · enantioselectivity · surface chemistry

[1] D. Stacchiola, L. Burkholder, W. T. Tysoe, *J. Am. Chem. Soc.* **2002**, *124*, 8984.
[2] A. M. Berg, D. L. Patrick, *Angew. Chem.* **2005**, *117*, 1855; *Angew. Chem. Int. Ed.* **2005**, *44*, 1821.
[3] J. A. Switzer, H. M. Kothari, P. Poizot, S. Nakanishi, E. W. Bohannan, *Nature* **2003**, *425*, 490.
[4] S. M. Barlow, R. Raval, *Surf. Sci. Rep.* **2003**, *50*, 201.
[5] C. F. McFadden, P. S. Cremer, A. J. Gellman, *Langmuir* **1996**, *12*, 2483.
[6] D. S. Sholl, *Langmuir* **1998**, *14*, 862.
[7] A. Ahmadi, G. Attard, J. Feliu, A. Rodes, *Langmuir* **1999**, *15*, 2420.
[8] D. S. Sholl, A. Asthagiri, T. D. Power, *J. Phys. Chem. B* **2001**, *105*, 4771.
[9] R. M. Hazen, D. S. Sholl, *Nat. Mater.* **2003**, *2*, 367.
[10] J. D. Horvath, A. Koritnik, P. Kamakoti, D. S. Sholl, A. J. Gellman, *J. Am. Chem. Soc.* **2004**, *126*, 14988.
[11] X. Y. Zhao, R. G. Zhao, W. S. Yang, *Langmuir* **2000**, *16*, 9812.
[12] R. M. Hazen, T. R. Filley, G. A. Goodfriend, *Proc. Natl. Acad. Sci. USA* **2001**, *98*, 5487.
[13] T. D. Power, A. Asthagiri, D. S. Sholl, *Langmuir* **2002**, *18*, 3737.
[14] Z. Sljivancanin, K. V. Gothelf, B. Hammer, *J. Am. Chem. Soc.* **2002**, *124*, 14789.
[15] A. J. Gellman, J. D. Horvath, M. T. Buelow, *J. Mol. Catal. A* **2001**, *167*, 3.
[16] J. D. Horvath, A. J. Gellman, *J. Am. Chem. Soc.* **2001**, *123*, 7953.
[17] J. D. Horvath, A. J. Gellman, *J. Am. Chem. Soc.* **2002**, *124*, 2384.
[18] P. Kamakoti, J. Horvath, A. J. Gellman, D. S. Sholl, *Surf. Sci.* **2004**, *563*, 206.
[19] D. Stacchiola, L. Burkholder, T. Zheng, M. Weinert, W. T. Tysoe, *J. Phys. Chem. B* **2005**, *109*, 851.
[20] R. B. Rankin, D. S. Sholl, *Surf. Sci.* **2004**, *548*, 301.
[21] R. B. Rankin, D. S. Sholl, *Surf. Sci.* **2005**, *574*, L1.
[22] X. Y. Zhao, S. S. Perry, *J. Mol. Catal. A* **2004**, *216*, 257.
[23] M. Giesen, S. Dieluweit, *J. Mol. Catal. A* **2004**, *216*, 263.
[24] A. Asthagiri, P. J. Feibelman, D. S. Sholl, *Top. Catal.* **2002**, *18*, 193.
[25] X. Li, A. J. Gellman, D. S. Sholl, *J. Mol. Catal. A* **2005**, *228*, 77.
[26] G. Kresse, J. Hafner, *Phys. Rev. B* **1993**, *48*, 13115.
[27] G. Kresse, J. Furthmuller, *Comput. Mater. Sci.* **1996**, *6*, 15.

